Sindh Univ. Res. Jour. (Sci. Ser.) Vol. 50 (3D) 18-23 (2018)

SINDH UNIVERSITY RESEARCH JOURNAL (SCIENCE SERIES)

Inductive Resonant Power Transfer and Topology Consideration

I. ADAM++, S. KHAN*, A. N. NORDIN*, K. N. BADRON*, H. MANSOR*, K. A. KADIR++

University of Kuala Lumpur, Malaysia, International Islamic University of Malaysia

Received 10th June 2018 and Revised 15th September 2018

Abstract: This paper aims to study the performance of all basic inductive resonant wireless power transfer (WPT) topologies for power transfer efficiency, using the effect of circuit topology in affecting the coefficient of coupling. In the study, all the four basic inductive resonant wireless power transfer topologies are analyzed and simulated. The simple T-equivalent circuit is used to represent the system and MATLAB® are used as the backbone of the analysis. The analysis shows that the parallel-to-series and parallel-to-parallel topology configurations give the best power transfer efficiency. The results show that parallel to series and parallel to parallel average power transfer efficiency referring to coefficient coupling (k) are 81% and 80% respectively, compared to the series-to-parallel and series-to-series which are almost 70% accordingly. The study provides evidence of further system analysis for parallel to series and parallel-to-parallel WPT topologies. The results of the analysis would prove useful in furthering insight into its application such wireless battery charging of electric vehicles.

Keywords: Wireless power transfer (WPT); power transfer efficiency; electric vehicle.

1. INTRODUCTION

In metropolitan cities, fossil fuel based vehicles emissions are realized as major concerns. Concerned authorities setting targets by which for CO2 emissions are to be reduced lay down regulations. Traffic jams are another major concern and at a number of traffic hot spots walking would be preferable to drive, and many roads are in planning to become walkways. It is expected that the hybrid electric vehicles, plug-in electric vehicles, and battery electric vehicles would soon become standard means of transport, banning possible altogether CO2 emission-based transport into the cities. As the result, the walkways of the futuristic cities need be fitted with charging stations for electric vehicles. In addition, the gradual increases of electrical vehicles are sure to be associated with a gradual increase of wireless battery charging compared to wireless charging or plug-in electric vehicle. For that reason, wireless power transfer (WPT) has been gaining an ever-increasing attention due to the convenience it offers compared to wired means of battery charging.

Fig. 1 shows the concept of wireless power transfer, consisting the transmitting and the receiving ends. As shown, the wire is eliminated in conveying the power to the load. In the case of radio frequency or microwave, the antenna is used to transfer the power, however, in field coupling approach, it is either the magnetic or electric field that gets coupled as a link for power transfer through coupling devices such capacitor or inductor.

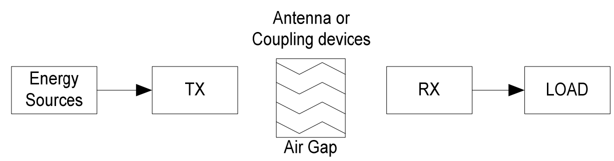

Fig. 1: Non-contact Wireless Power Transfer System

Currently, most of the electronic devices are powered by batteries, which need to be recharged very often (*Schlierf et al.,* 2007). This fact motivated the researchers in devising means enabling wireless powering of these and similar devices in a sort of applications, such as electronic portable devices, electric vehicles, biomedical devices, and consumer electronics (Jiang *et al.,* 2013). In addition, the demand for WPT technology is increasing continuously as more consumers are increasing the use of portable devices (Johari *et al.,* 2014).

Power transfer efficiency and distance coverage are the main concern in the existing as well as newly developed WPT system. At the moment, the limitation of the wireless power transfer is high cost, low efficiency, sensitive to coil alignment, large size and limited in the distance (*Khan et al.,* 2012). For that reason, the WPT technology requires novel designs, novel topologies, novel methods, new materials as well as new control methods. In general, power transfer efficiency and distance coverage are the main concern in the existing as well as newly developed WPT system.

++ Corresponding author: Ismail Adam email: i.adam.mlk@gmail.com
*Electronics & Electrical Sections, University of Kuala Lumpur, Malaysia,

The inductive coupling and capacitive coupling have been two main methods for wireless power transfer (ICNIRP, 1998). The capacitive coupling method is more sensitive and complex for wireless power harvesting system (Kurs *et al.,* 2012). Almost all of the newly WPT technologies have been using inductive coupling as the main approach in their design due to the nature of comfortable implementation. Inductive coupling provides better transfer efficiency at very short distances and degrades by distance increased so that it can able to perform well and safely for certain meters (Arsad *et al.,* 2012). These parameters can be improved by adopting the resonance principle based inductively coupled coils in the system (Torla *et al.,* 2013). It is reported that the magnetic resonant coupling WPT systems transmit longer transmission distances compared to the inductive coupling WPT systems (Nataraj *et al.,* 2016). For that reason, the magnetic resonant coupling or inductive resonant WPT systems have been adopted for this study.

In move-and-charge application, such charging of moving the electrical cart, the impact of misalignment and distance between TX and RX on power transfer has attracted many researchers. The number of solutions which focus particularly on transmitting and receiving coil structures, shapes and materials have been proposed (*Chang et al.,* 2013). In (*Li et al.,* 2016), the factors that determine the power transfer efficiency were discussed based on the capacitor compensation technique to maintain the Q-factor of the system. While in this project, the novel technique in estimating the actual resonance frequency for a given coupling coefficient (k) will be developed. This ensures the highest possible power transfer is achieved even at a lower coupling coefficient (k) [provided not 0]; as well maintains the Q-factor of the system. For that purpose, the highest power efficiency and the most stable power transfer topology will be analyzed and choose as the platform of the system. Therefore, the power transfer performance of the inductive resonant WPT systems from topology viewpoint using circuit-modeling approach is analyzed in this paper.

2. BACKGROUND

In this section, the conversion of the magnetically coupled circuits to the T-equivalent circuit of series-to-series will be discussed in details. The technique is furthered used in deriving the system equivalent for series-to-parallel, parallel-to-series and parallel-to-parallel topologies.

2.1 T-equivalent Circuit Modelling of series-to-series topology

The equivalent circuit of the magnetically coupled circuit is shown in Fig. 2. As shown, the circuit is coupled via the mutual inductance (M) of some like transformer. R1 and R2 are the coil resistances which are normally small and can be ignored in the application.

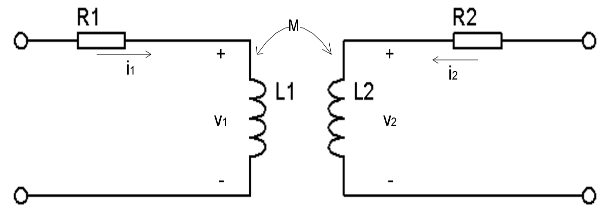

Fig. 2: Equivalent circuit of the magnetically coupled circuit

The input and output terminal voltages of Fig. 2 can be written as

$$v_1 = L_1 \frac{di_1}{dt} + M \frac{di_2}{dt} \tag{1}$$

$$v_2 = M \frac{di_1}{dt} + L_2 \frac{di_2}{dt} \tag{2}$$

By using (1) and (2), the magnetically coupled circuit of Fig. 2, can be rearranged into an equivalent circuit as shown in Fig. 3.

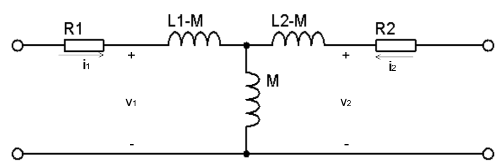

Fig. 3: The T-equivalent circuit for the magnetically coupled circuit

In general, **(Fig. 3)** represents the T-equivalent circuit for the magnetically coupled circuit. This equivalent circuit of Fig. 3, is used throughout conversion for all the four inductive resonant WPT studied for system analysis. As an example of conversion of the magnetically coupled circuit to its equivalent T network is shown in below.

Fig.4 (a) shows the series-to-series inductive resonant WPT circuit. This circuit is called series-to-series due to the primary capacitor (CS) is in series with a primary inductor (L1), and the secondary capacitor(CO) is in series with a secondary inductor (L2). The conversion is done by replacing the components in the red dotted block to the T-equivalent circuit for the magnetically coupled circuit of Fig. 3. This is shown in **(Fig. 4 (b).**

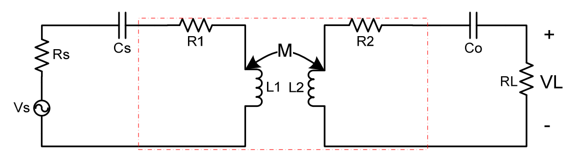

Fig. 4: (a) Series-to-series magnetically coupled Network into T-equivalent

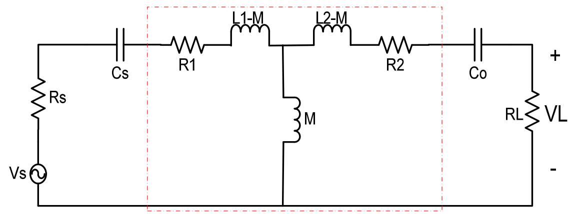

Fig. 4: (b) T-equivalent circuit

The mathematical derivation of the system parameters such input current of all the four basics inductive resonant WPT topologies is derived by denoting the current flow in the loops as the example shown in series to the series topology in Fig.5.

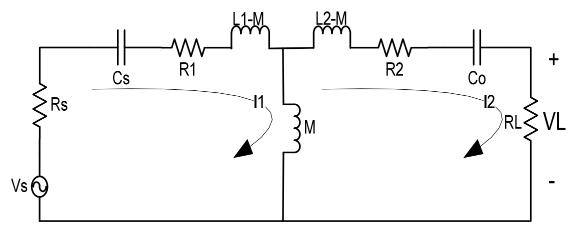

Fig. 5: Series-to-series T-equivalent circuit

It is easy to write the From Fig. 5, the loop equations for the circuit can be written as

$$\begin{bmatrix} v_s \\ 0 \end{bmatrix} = \begin{bmatrix} rs - j\dfrac{1}{\omega Cs} + R_1 + j\omega L_1 & -j\omega M \\ -j\omega M & R_L + R_2 + j\omega L_2 - j\dfrac{1}{\omega Co} \end{bmatrix} \begin{bmatrix} I_s \\ I_L \end{bmatrix} \tag{3}$$

From (3), the determinants can be derived as

$$\Delta = \left(rs - j\frac{1}{\omega Cs} + R_1 + j\omega L_1 \right)\left(R_L + R_2 + j\omega L_2 - j\frac{1}{\omega Co} \right) + \omega^2 M^2$$

$$\Delta I_S = v_S \left(R_L + R_2 + j\omega L_2 - j\frac{1}{\omega Co} \right)$$

$$\Delta I_L = -j\omega M v_S$$

Finally, by using crammer's rule, the input current, output current, input power and output power can be written such as (4) - (7).

$$I_s = \frac{v_S\left(R_L + R_2 + j\omega L_2\right)}{\left(rs + R_1 + j\omega L_1\right)\left(rs + R_2 + j\omega L_2\right) + \omega^2 M^2} \tag{4}$$

$$I_L = \frac{-j\omega M v_s}{\left(rs + R_1 + j\omega L_1\right)\left(rs + R_2 + j\omega L_2\right) + \omega^2 M^2} \tag{5}$$

$$P_I = v_s \times I_S \tag{6}$$

$$P_O = I_L^2 R_L \tag{7}$$

2.2 Parallel-to-parallel Topology

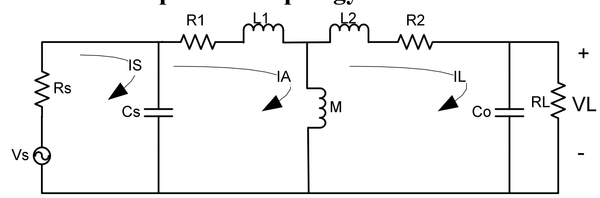

Fig. 6: Parallel-to-parallel T-equivalent circuit

From Fig.6, let the parallel impedance (ZL) of Co and RL is written as

$$Z_L = R_L \parallel \left(-j\frac{1}{\omega Co} \right) = \frac{R_L \times \left(-j\dfrac{1}{\omega Co} \right)}{R_L + \left(-j\dfrac{1}{\omega Co} \right)}$$

The loop equation of Fig. 6 can be written as

$$\begin{bmatrix} vs \\ 0 \\ 0 \end{bmatrix} = \begin{bmatrix} rs - j\dfrac{1}{\omega Cs} & j\dfrac{1}{\omega Cs} & 0 \\ j\dfrac{1}{\omega Cs} & R_1 + j\omega L_1 + j\omega M - j\dfrac{1}{\omega Cs} & -j\omega M \\ 0 & -j\omega M & R_2 + j\omega L_2 + j\omega M + Z_L \end{bmatrix} \begin{bmatrix} I_S \\ I_a \\ I_L \end{bmatrix}$$

and the determinants can be written as

$$\Delta = \left(rs - j\frac{1}{\omega Cs} \right)\left(\left(R_1 + j\omega L_1 + j\omega M - j\frac{1}{\omega Cs} \right)\left(R_2 + j\omega L_2 + j\omega M + Z_L \right) + \omega^2 M^2 \right)$$
$$- j\frac{1}{\omega Cs}\left(j\frac{1}{\omega Cs} \times \left(R_2 + j\omega L_2 + j\omega M + Z_L \right) \right)$$

$$\Delta I_S = v_S \left(\left(R_1 + j\omega L_1 + j\omega M - j\frac{1}{\omega Cs} \right)\left(R_2 + j\omega L_2 + j\omega M + Z_L \right) + \omega^2 M^2 \right)$$

$$\Delta I_L = v_S \frac{M}{Cs}$$

2.3 Series-to-parallel Topology

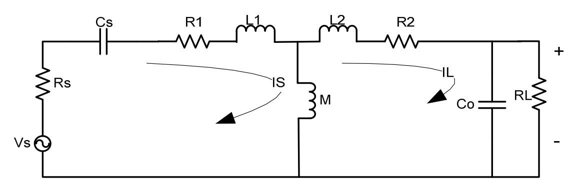

Fig. 7: Series-to-parallel T-equivalent circuit

The T-equivalent circuit of series-to-series is shown in Fig.7, the loop equation can be written as

$$\begin{bmatrix} v_s \\ 0 \end{bmatrix} = \begin{bmatrix} rs + R_1 - \dfrac{j}{\omega Cs} + j\omega L_1 & -j\omega M \\ -j\omega M & R_2 + j\omega L_2 + R_L \parallel -j\dfrac{1}{\omega C_O} \end{bmatrix} \begin{bmatrix} I_s \\ I_L \end{bmatrix}$$

and the determinants can be written as

$$\Delta = \left(rs + R_1 - \frac{j}{\omega Cs} + j\omega L_1 \right)\left(R_2 + j\omega L_2 + R_L \parallel -j\frac{1}{\omega C_O} \right) + \omega^2 M^2$$

$$\Delta I_S = v_S\left(R_2 + j\omega L_2 + R_L - j\frac{1}{\omega C_O}\right)$$

$$\Delta I_L = -j\omega M v_S$$

2.3 Parallel-to-series Topology

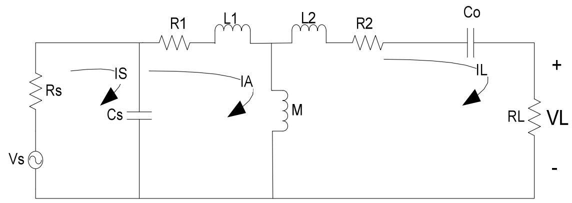

Fig. 8: Parallel-to-series T-equivalent circuit

The T-equivalent circuit of parallel-to-series is shown in Fig.8, the loop equation can be written as

$$\begin{bmatrix} vs \\ 0 \\ 0 \end{bmatrix} = \begin{bmatrix} rs - j\frac{1}{\omega Cs} & j\frac{1}{\omega Cs} & 0 \\ j\frac{1}{\omega Cs} & R_1 + j\omega L_1 + j\omega M - j\frac{1}{\omega Cs} & -j\omega M \\ 0 & -j\omega M & R_2 + j\omega L_2 + j\omega M + R_L - j\frac{1}{\omega Co} \end{bmatrix} \begin{bmatrix} I_S \\ I_a \\ I_L \end{bmatrix}$$

and the determinants can be written as

$$\Delta = \left(rs - j\frac{1}{\omega Cs}\right) \times \left(\left(R_1 + j\omega L_1 + j\omega M - j\frac{1}{\omega Cs}\right)\left(R_2 + j\omega L_2 + j\omega M + R_L - j\frac{1}{\omega Co}\right) + \omega^2 M^2\right)$$
$$-j\frac{1}{\omega Co} \times \left(\left(R_2 + j\omega L_2 + j\omega M + R_L - j\frac{1}{\omega Co}\right) + \omega^2 M^2\right)$$

$$\Delta I_S = v_S\left(\left(R_1 + j\omega L_1 + j\omega M - j\frac{1}{\omega Cs}\right)\left(R_2 + j\omega L_2 + j\omega M + R_L - j\frac{1}{\omega Co}\right) + \omega^2 M^2\right)$$

$$\Delta I_A = v_S\left(rs - j\frac{1}{\omega Cs}\right)\left(R_2 + j\omega L_2 + j\omega M + R_L - j\frac{1}{\omega Co}\right)$$

$$\Delta I_L = v_S \frac{1}{\omega Cs}\omega M = v_S \frac{M}{Cs}$$

3. METHODS AND RESULTS

In this section, we discuss the methods utilized in analyzing the power transfer and coupling coefficient (k) relationship of series-to-series, series-to-parallel, parallel-to-series and parallel-to-parallel topologies. Subsequently, the simulation results of all topologies will be presented and discussed.

3.1 The MATLAB Simulation

Referring to the T-equivalent circuits such as Fig. 5, the value of Rs, R1, R2, RL, L1, L2, Cs and Co are set to 5Ω, 1Ω, 1Ω, 10Ω, 100µH, 100µH, 10µF and 10µF respectively. The MATLAB simulation is done by sweeping the frequency from 0 Hz to 1 kHz in steps of 1Hz for a circuit with coupling coefficient (k) ranging from 0 up to 1 in step of 0.05 per iteration. The output power equations for all topologies were used in the simulation. The data for all simulation is transferred into a worksheet for temporary and another MATLAB® source code is developed to further analyze the power transfer properties of the circuits. All of the results are presented below.

3.2 Power Transfer of series-to-series Topology

The power transfer against the coupling coefficient (k) plot of series-to-series topology is shown in Fig.9. As expected, the power transfer efficiency is increased by the by increasing the coupling coefficient (k). The average power transfer efficiency for the coupling coefficient (k) of 0.3 is about is 31%. The average power transfer efficiency parallel-to-parallel topology is found to be 72%.

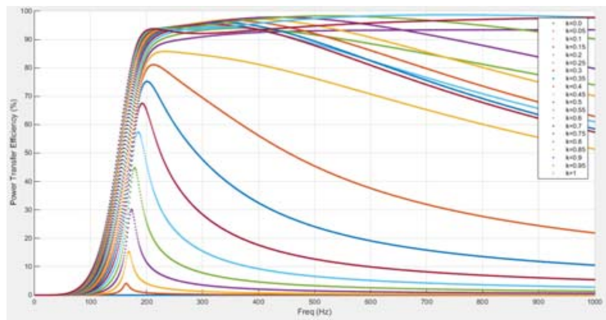

Fig. 9: Power transfer against coupling coefficient (k) plot of series-to-series topology

3.3 Power Transfer of parallel-to-parallel Topology

The power transfer against the coupling coefficient (k) plot of parallel-to-parallel topology is shown in Fig.10. As expected, the power transfer efficiency is increased by the by increasing the coupling coefficient (k). The average power transfer efficiency for the coupling coefficient (k) of 0.3 is about is 55%. The average power transfer efficiency parallel-to-parallel topology is found to be 80%.

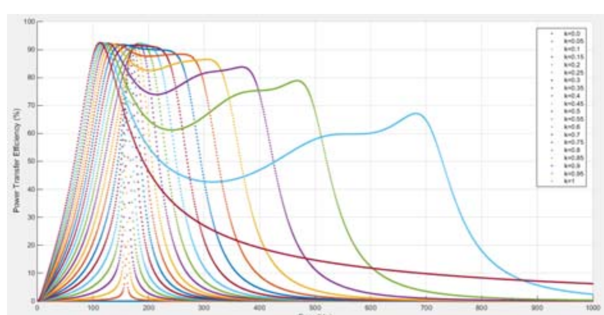

Fig. 10: Power transfer against coupling coefficient (k) plot of parallel-to-parallel topology

3.4 Power Transfer of series-to-parallel Topology

The power transfer against the coupling coefficient (k) plot of series-to-parallel topology is shown in Fig.11. As in series-to-series topology, the power transfer efficiency is increased by the by increasing the coupling coefficient (k). The average power transfer efficiency for the coupling coefficient (k) of 0.3 is about is 56%. The average power transfer efficiency of series-to-parallel topology is found to be 81%.

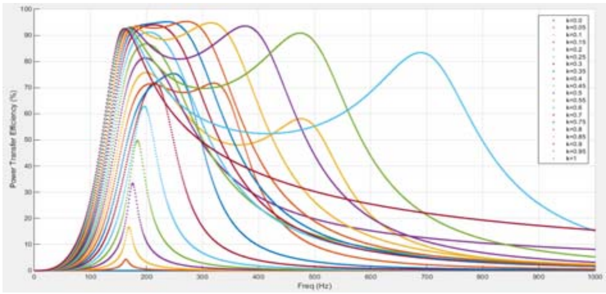

Fig 11: Power transfer against coupling coefficient (k) plot of series-to-parallel topology

3.5 Power Transfer of parallel-to-series Topology

The power transfer against the coupling coefficient (k) plot of parallel-to-series topology is shown in Fig.12. As expected, the power transfer efficiency is increased by increasing the coupling coefficient (k).

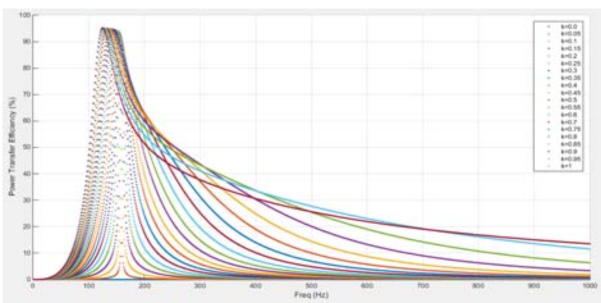

Fig. 12: Power transfer against coupling coefficient (k) plot of parallel-to-series topology

The average power transfer efficiency for the coupling coefficient (k) below 0.3 is about 55%, and the average power transfer efficiency parallel-to-parallel topology is found to be 80%.

4. DISCUSSION

From the power transfer against coupling coefficient (k) of all topologies in Fig. 9 to Fig. 12, the power transfer efficiency against the coupling coefficient of all four topologies is plotted such in Fig.13.

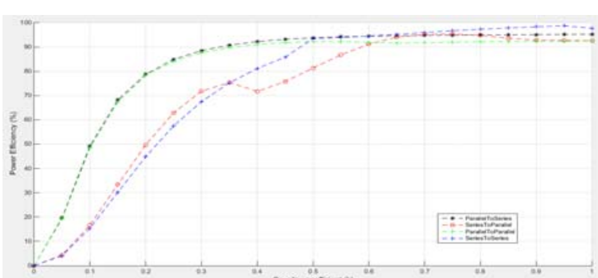

Fig. 13: Power transfer efficiency against coupling coefficient (k) plot of 4 basic inductive resonant wireless power transfer topologies

It is clear, the maximum power transfer efficiency is achieved at coupling coefficient (k) equal to 1. At a glance, the parallel to series topology shows the best power transfer efficiency over the other three topologies. In detail, the parallel to series topology produced the average power transfer of 81% for k varies from 0 to 1; and 56% for k varies from 0 to 0.3.

Topologies	Average power (k varies from 0 to 0.3)	Average power (k varies from 0 to 1)
parallel-to-series	56%	81%
series-to-parallel	34%	70%
parallel-to-parallel	55%	80%
series-to-series	31%	72%

Table-1: Differences average power transfer for all four inductive resonant WPT topologies

(Table -1): lists the average power of all topologies for varying k. It shown that the parallel-to-series topology provides the highest average power transfer efficiency at k varies from 0 to 0.3 and from k varies from 0 to 1 respectively.

5. CONCLUSION

In order to achieve the objective of this study which is to analyze the power transfer performance of basic topologies of the inductive resonant WPT system, some experimental steps are followed. The first step is converting the inductive resonant WPT magnetically coupled circuits into their equivalent T-networks. Then, all the interest parameters such input current are derived by using Crammer's rule for simplicity. The analysis is furthered done by using the MATLAB ® simulation package assisted by Excel worksheet for temporary data storage. The power transfer of each four inductive resonant WPT topologies against frequency with varying coefficient coupling were plotted for individual analysis. The plots show that the maximum power transfer can be achieved at a coupling coefficient of 1, and for each of the coupling coefficient tested there is a slight shifting of frequency at which the power transfer is optimum. This study shows that the parallel-to-series are preferable to other inductive resonant WPT topologies. It produces the highest power transfer efficiency at k varied from 0 to 1. The study provides the evidence that the parallel-to-parallel and parallel-to-series topologies are worth for further study of the WPT based on the inductive resonant technique. Further analysis of the relationship of input impedance to the optimum frequency and effect of varying load impedance to the power transfer efficiency will be done.

REFERENCES:

Arsad, A., S. Khan, Z.Alam, A. H. M. Tasnim, R. Gunawan, T. D. Ahmad, R. Nataraj, C. An Activity (2016) Monitoring System for Senior Citizens Living Independently Using Capacitive Sensing Technique. IEEE Int. Instrum. Meas. Technol. Conf., no. 1, 449–454.

Chang, Z, K. T. Chau, (2015) Homogeneous Wireless Power Transfer for Move-and-Charge. IEEE Transactions on Power Electronics, vol. 30, no. 11, 6213-6220.

International Commission on Non-Ionizing Radiation Protection. (1998) ICNIRP Guidelines for Limiting Exposure To Time-Varying Guidelines for Limiting Exposure To Time-Varying Electric, Magnetic and Electromagnetic fields. Health Phys., vol. 74, 494-522.

Jiang, H., J. Zhang, Lan, Di. Chao, Kelvin K. Shahnasser, K. Fechter, R. Hirose, S. Harisson, M. R. Shuvo. (2013) A Low- Frequency Versatile Wireless Power Transfer Technology for Biomedical Implants. *IEEE Trans. on Biomedical circuits and systems*, vol. 7, no. 4, 526–535.

Johari, R., J. V. Krogmeier, D. J. Love, (2014) Analysis and practical considerations in implementing multiple transmitters for wireless power transfer via coupled magnetic resonance. *IEEE Trans. Ind. Electron.*, vol. 61, no. 4, 1774–1783

Khan, I. M., S. Khan, O. O. Khalifa, (2012) Wireless Transfer of Power to Low Power Implanted Biomedical Devices: Coil Design Considerations. *IEEE Int. Instrum. Meas. Tech* nol. Conf., no. 1, 2584–2588.

Kurs, A., A.Karalis, R. Moffatt, J. D Joannopoulos,. P.Fisher, M.Soljacic, M. Soljac, (2009) Wireless Power Transfer via Strongly Coupled Magnetic Resonances. Science (80)., vol. 83, no. 6Pp.

Li, Q. Y. C. Lian, (2016) An Inductive Power Transfer System with a High-Q Resonant Tank for Mobile Device Charging. IEEE Transactions on Power Electronics, vol. 30, no. 11, 6203-6212.

Nataraj, C., S. Khan, M. H. Habaebi, A.Ashad, (2016) Resonant Coils Analysis for Inductively Coupled Wireless Power Transfer Applications. IEEE Int. Instrum. Meas. Technol. Conf., no. 1, 109–114.

Schlierf, R., U. Horst, M. Ruhl, T. Schmitz-Rode, W. Mokwa, U. Schnakenberg, (2007) A fast telemetric pressure and temperature sensor system for medical applications. *J. Micromechanics Microengineering*, vol. 17, no. 7, 98–102.

Torla, A. L., S. Khan, A. G. Muthalif, A. W. Azman, Y. M. Mustafah, (2013) Low voltage DC power supply with spike-blocking features," IEEE Int. Instrum. Meas. Technol. Conf., 1161–1164.